The American Journal of Human Genetics

Supplemental Data

Intra-mitochondrial Methylation Deficiency Due to Mutations in *SLC25A26*

Yoshihito Kishita, Aleksandra Pajak, Nikhita Ajit Bolar, Carlo M.T. Marobbio, Camilla Maffezzini, Daniela V. Miniero, Magnus Monné, Masakazu Kohda, Henrik Stranneheim, Kei Murayama, Karin Naess, Nicole Lesko, Helene Bruhn, Arnaud Mourier, Rolf Wibom, Inger Nennesmo, Ann Jespers, Paul Govaert, Akira Ohtake, Lut Van Laer, Bart L. Loeys, Christoph Freyer, Ferdinando Palmieri, Anna Wredenberg, Yasushi Okazaki, and Anna Wedell

Supplemental Note: case reports

The studies were approved by the regional Ethics Committees at Karolinska Institutet, Sweden, the Saitama Medical University, Japan and Antwerp University Hospital, Belgium. Written informed consent was obtained from the parents.

Individual 1

Individual 1 (P1) was born 2009 in gestational week 39 to consanguineous healthy parents from Iraq. There is one healthy sister born 2006. Pregnancy and neonatal period were normal. Birth weight was 3360 grams, length 53 cm and head circumference 35.5 cm. The boy presented at 4 weeks with acute circulatory collapse and pulmonary hypertension, requiring extra-corporeal membrane oxygenation for 5 days. Urinary organic acid analysis showed increased excretion of lactate, 3-methyl-glutaconic acid and alpha-ketoglutarare but was otherwise normal. There was severe lactic acidosis around 20 mmol/L (ref 0.5-2.3). Sodium dichloroacetic acid had good effect, and the boy slowly normalized. Plasma lactate has since been intermittently slightly elevated but most often within the normal range. Plasma glycine was increased up to 617 μmol/L (ref 80-320) at 5 weeks. Analyses of urinary amino acids, urinary purines and pyrimidines, and plasma acylcarnitines gave normal results.

A lung biopsy performed at 5 weeks showed slight interstitial oedema and muscularized arterioli compatible with pulmonary hypertension of unclear etiology, and discreet presence of hyperplastic pneumocytes and clear cells with increased glycogen, but no signs of capillary alveolar dysplasia, inflammation, or other abnormalities. Computer tomography (CT) of the chest and abdomen showed an enlarged right ventricle of the heart, wide *truncus pulmonalis* and prominent lung artery.

A muscle biopsy was performed at 8 weeks from the *tibialis anterior* muscle. Investigation of isolated muscle mitochondria revealed reduced activities of complex I and IV and reduced ATP production rate. In particular, ATP production was virtually absent using pyruvate as a substrate (Figure S1A and B). Gross muscle histology was unremarkable without any increase in centrally positioned nuclei and no signs of inflammation or increased glycogen content. There was an even ratio of type 1 and type 2 muscle fibres. Combined staining for SDH and COX revealed numerous COX-negative fibres (Figure S1C). There were no ragged red fibres and electron microscopy did not reveal any morphologically abnormal mitochondria. Blue native gel electrophoresis showed reduced amounts of complex I and IV of the respiratory chain (Figure S1D).

Sanger sequencing was performed of the complete mtDNA isolated from muscle and the *PDHA1*, *POLG*, and *TK2* genes from DNA isolated from blood, without positive findings.

At 3.5 years there was a second episode of pulmonary hypertension, which also normalized. An enlarged right atrium and ventricle of the heart was observed by echocardiogram. The boy was treated with sildenafil until 4 years 10 months of age. He has since been cardiopulmonary stable without this treatment.

At 6 years 3 months the boy has increasing muscle weakness, exercise intolerance and fatigue. He walks without support but only short stretches. He has severe problems with recurrent abdominal pain and lack of appetite, and development is slightly delayed.

Individual 2

Individual 2 (P2) was the first child of healthy Japanese parents. There is one healthy younger brother. The girl was born at 39 weeks of gestation. Her birth weight and height were 3076 g (+0.2 SD) and 48.2 cm (-0.7 SD). Apgar scores were 9 at 1 minute and 10 at 5 minutes. Around 11 hours after birth, she developed respiratory failure. Blood lactate was elevated at 41.8 mmol/L (ref <1.8) and showed severe acidosis (pH 6.6). Pyruvate levels were 0.65 mmol/L (ref <0.1). She required mechanical ventilation and peritoneal dialysis. Histology of a muscle biopsy specimen at 6 days indicated no ragged red fibers (RRF) but mild COX deficiencies were observed. There was no mutation in muscle mitochondrial DNA. Blood acylcarnitine analysis showed no abnormality. Urine organic acid analysis also showed no abnormality except for large amount of lactate. Amino acid profiles showed elevated alanine. At 133 days of age, she was discharged from hospital. Resting lactate levels in the blood was persistently high (4.4mmol/L) and acute infections caused an increase in blood lactate (>11.1mmol/L) despite treatment with vitamins, L-carnitine, coenzyme Q and dichloroacetic acid. She could walk at 1 year and her DQ score was 82 at 1 year and 10 months of age. When she was 2 years old, a remarkable hyperlacticacidemia (36.1 mmol/L) was observed, followed by cardiopulmonary arrest and hypoxic brain damage. After this episode she remained severely handicapped. A muscle biopsy was performed at 3 years and showed remarkable ragged RRF and COX deficiencies (Figure S1F). Respiratory chain enzyme activities were normal in fibroblasts but showed decreased complex I, III and IV activities in skeletal muscle (Figure S1E).

Individual 3

Individual 3 (P3), born to consanguineous parents of Moroccan decent, was delivered by caesarean section at 30 weeks 5 days after reduced fetal movements, polyhydramnios, fetal hydrops, and poor cardiotocography (CTG) were noted from 27 weeks of gestational age. She had normal antropometric parameters (birth weight 1300 grams, length 38 cm and head circumference 27.5 cm) but presented with poor Apgar score (3-5-6) due to bradycardia, hypotonia and respiratory insufficiency, necessitating assisted ventilation with high frequency oscillation. She suffered from lactic acidosis (84.6 mmol/L, ref 0.45-2.1 mmol/L) in CSF and urine (18 mmol/mmol creatinine, ref 1-285 μmol/mmol creatinine) and had elevated pyruvate levels (1.2 mmol/mmol

creatinine, ref 1-130 μmol/mmol creatinine) in urine. Brain ultra-sound demonstrated cystic necrosis of germinal matrix (extensive symmetrical caudothalamic germinolysis) and mild striatal arteriopathy. The child died of respiratory and multiple organ failure at 5 days of age. Measurement of respiratory chain activity in fibroblasts demonstrated decreased complex IV activity.

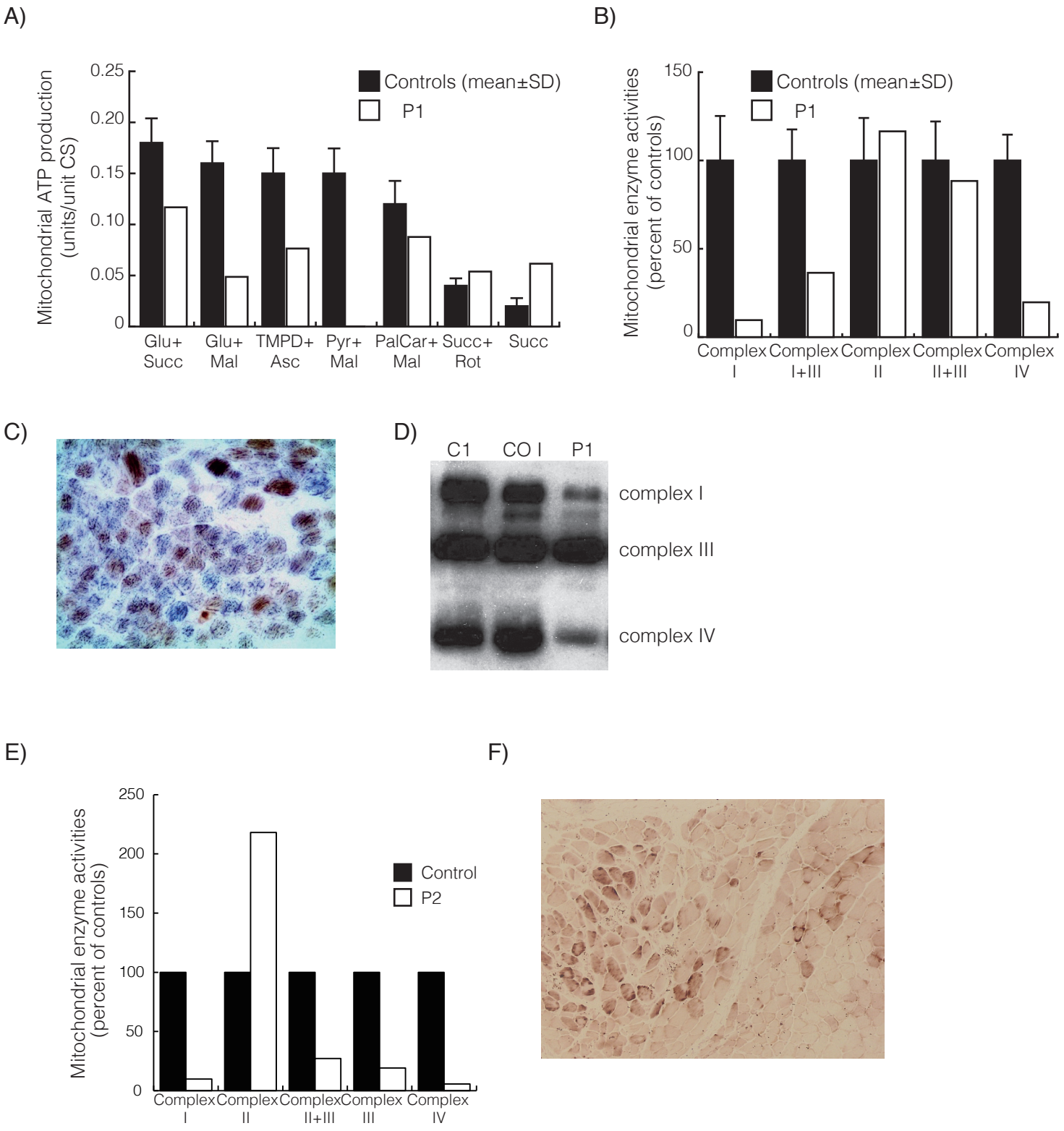

Figure S1: Bioenergetic analyses of mitochondria and muscle histology from individuals P1 and P2. A) Mitochondrial ATP production rate (MAPR) was determined by a firefly luciferase-based method at 25°C, using six different substrate combinations (Glu = glutamate; Succ = succinate; Mal = malate; TMPD = N,N,N',N'-Tetramethyl-p-phenylenediamine dihydrochloride; Asc = ascorbate; Pyr = pyruvate; PalCar = palmitoyl-L-carnitine; Rot = rotenone). Results are presented as the ATP synthesis rate (units) per unit of citrate synthase (CS) activity (control n=11; age 0–5 years). B) Respiratory chain enzyme activities of complex I (NADH:coenzyme Q reductase), complexes I and III (NADH:cytochrome *c* reductase), complex II (succinate dehydrogenase), complexes II and III (succinate:cytochrome *c* reductase, SCR), complex IV (COX) and CS were determined. Results are presented as percentage of mean control (n=9; age 0–5 years) values. The range of control values is depicted as ±SD. (C) cytochrome *c* - succinate dehydrogenase (COX-SDH) double staining of skeletal muscle from P1. (D) Blue-native PAGE followed by Western blot analysis of control (C1), individual with isolated complex I defect (CO I) and P1 skeletal muscle mitochondria. Antibodies against complex I, complex III and complex IV were used. (E) Respiratory chain enzyme activities as in (B) on P2 muscle mitochondria. (F) Cytochrome oxidase (COX) staining of skeletal muscle from 3 years old P2.

A)

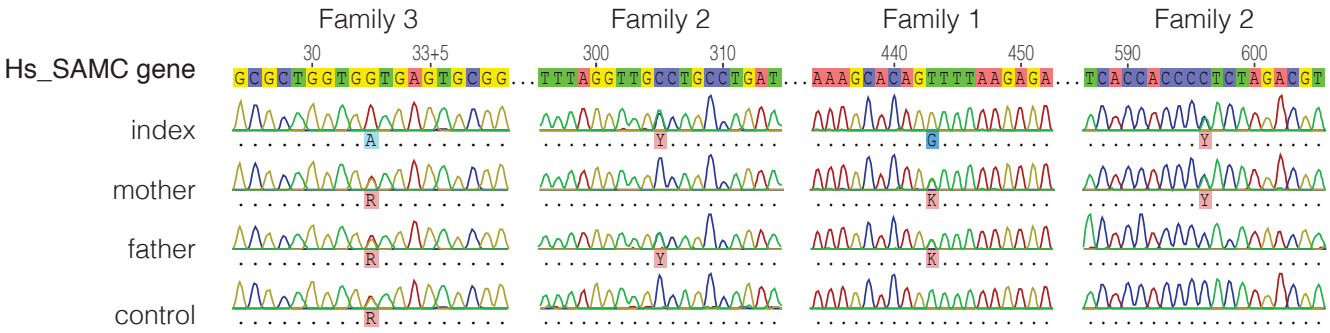

B)

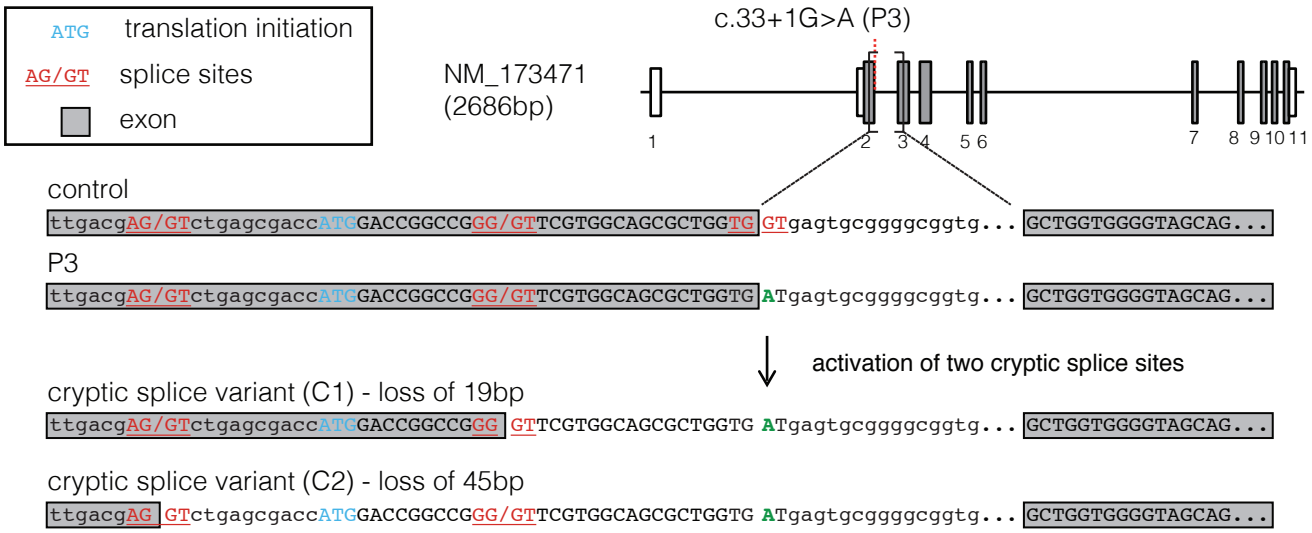

C)

Isoform	splice site used	% of clones indentified (n=48)	
		control	individual P3
P.1	wild type consensus	63.5	0
P.1	cryptic splice site 1 (C1)	0	31.2
P.1	cryptic splice site 2 (C2)	0	54.2
S.1	wild type consensus	36.5	0
S.1	cryptic splice site 1 (C1)	0	0
S.1	cryptic splice site 2 (C2)	0	10.5
S.1	other*	0	4.1

* two other splice isoforms of downstream regions following the UTR of the shorter isoform (S.1) were detected.

Figure S2: Electropherogram from Sanger sequencing results aligned to *SLC25A26*. (A) Fibroblast or blood DNA from family members were used for Sanger sequencing of *SLC25A26* (NM_173471.3). Control sample of family 1 is the unaffected sibling. (B) Schematic diagram showing the cryptic splice variants generated by the c.33+1G>A mutation in P3. (C) Cloning and sequencing of *SLC25A26* splice variants C1 and C2. PCR products from cDNA from control and P3 fibroblasts were cloned into pCRII TOPO vector (Invitrogen) and sequenced to determine the appropriate splice variant. Total number of clones sequenced (n=48).

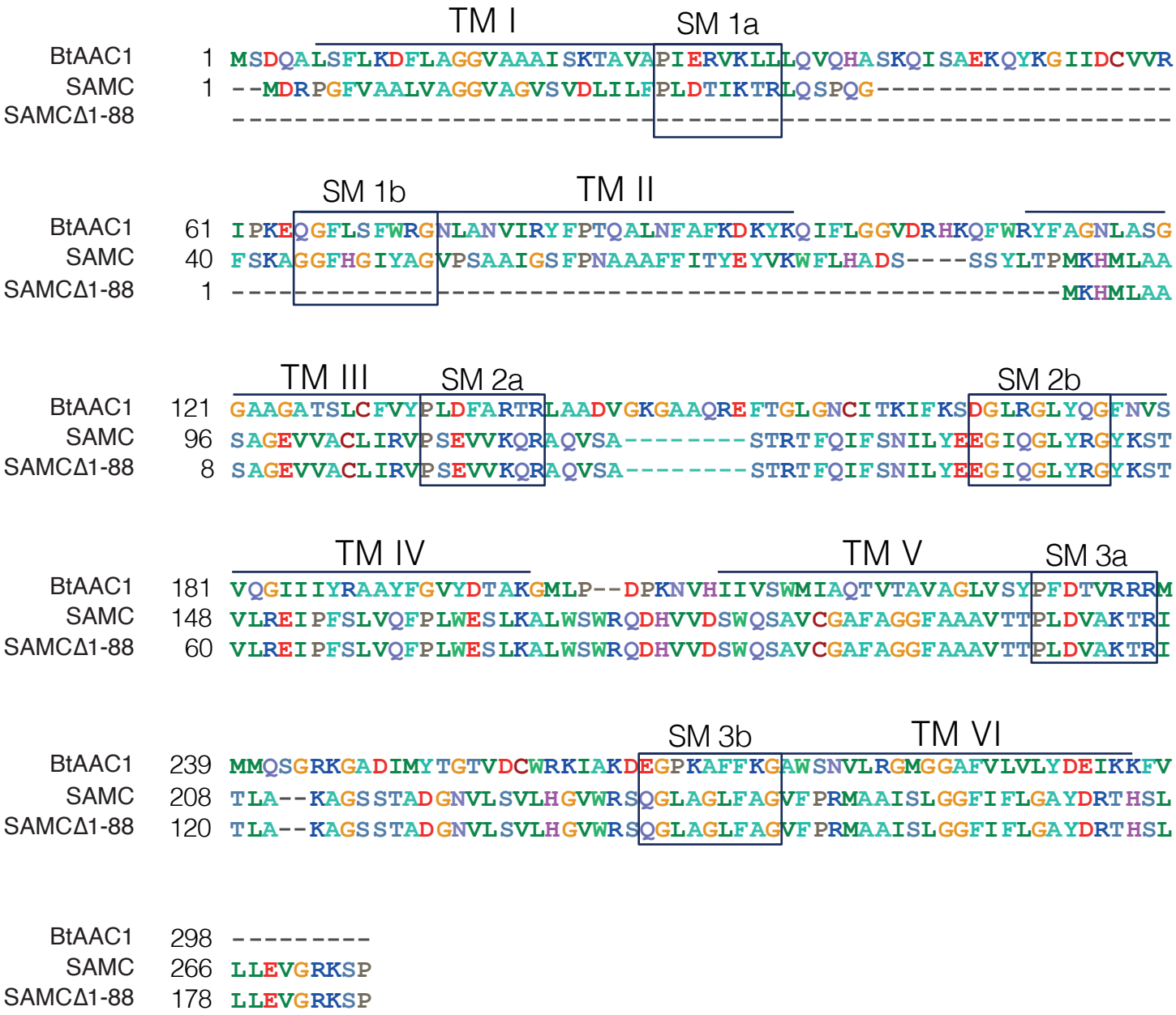

Figure S3. Alignments of the bovine ADP/ATP carrier (BtAAC1), SAMC and SAMCΔ1-88. The six transmembrane a-helices (TM I - TM VI) are linked by hydrophilic segments. The three signature motifs (SM1-SM3) present in the primary structure of the mitochondrial carriers are highlighted.

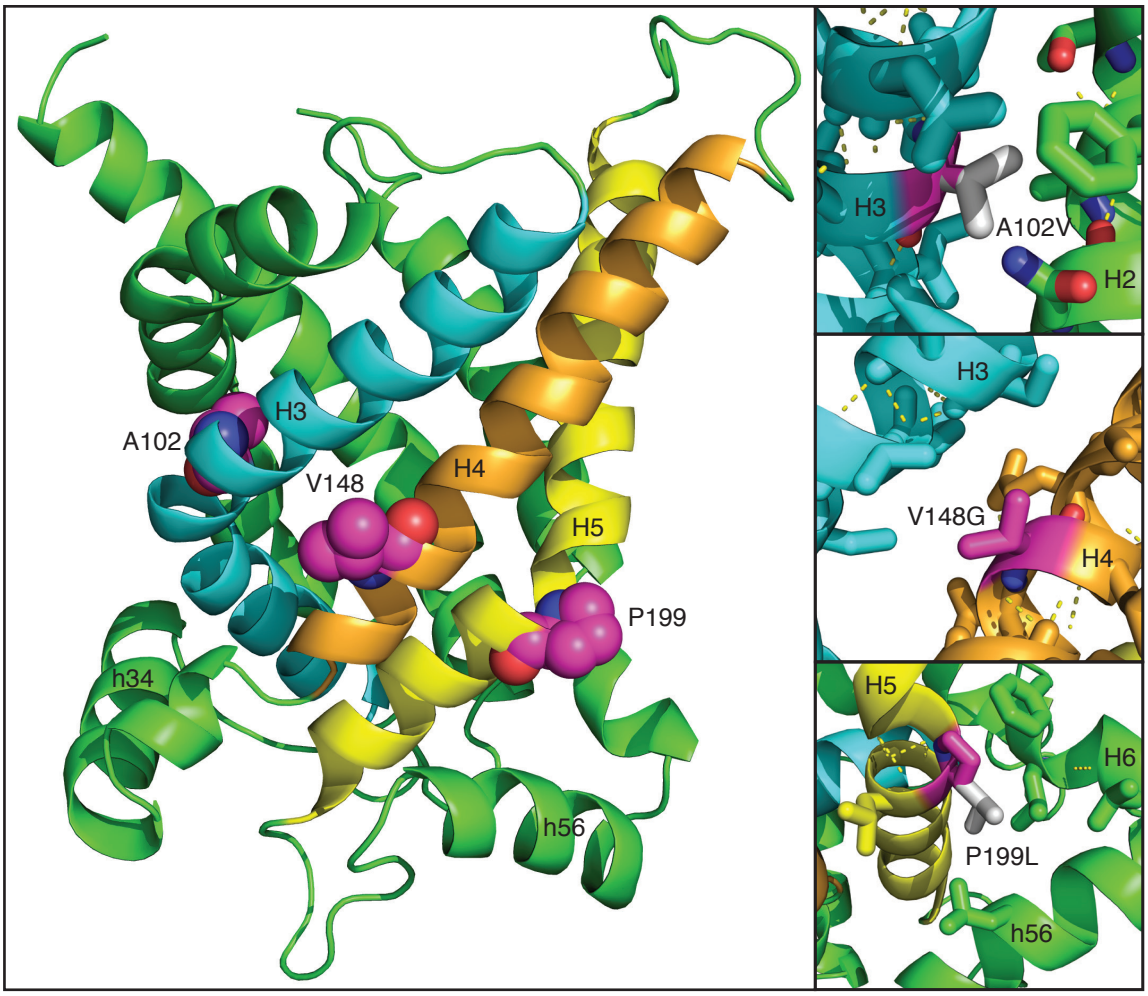

Figure S4: Structural homology model of SAMC illustrating the position of the p.Ala102Val, p.Val148Gly and p.Pro199Leu mutations. The homology model of human SAMC was made with MODELLER by using the carboxyatractyloside-inhibited ADP/ATP carrier structure (PDB ID 1OKC) as a template. The left panel shows the SAMC homology model in cartoon from a lateral view in the membrane plane with transmembrane α-helices H3, H4 and H5 in cyan, orange and yellow, respectively, and the rest of the molecule in green. The mutated residues are shown as spheres in magenta. The right panels show the mutated residues (magenta) and the replacing residues present in the SAMC mutants (white) as sticks at their positions. A102 is located at the interface between transmembrane α-helices H2 and H3. The side chain of V148 protrudes from transmembrane α-helix H4 towards the membrane. P199 creates a kink in transmembrane α-helix H5 in the cytoplasmic conformation of the carrier and its side chain is positioned towards matrix α-helix h56 and transmembrane α-helix H6.

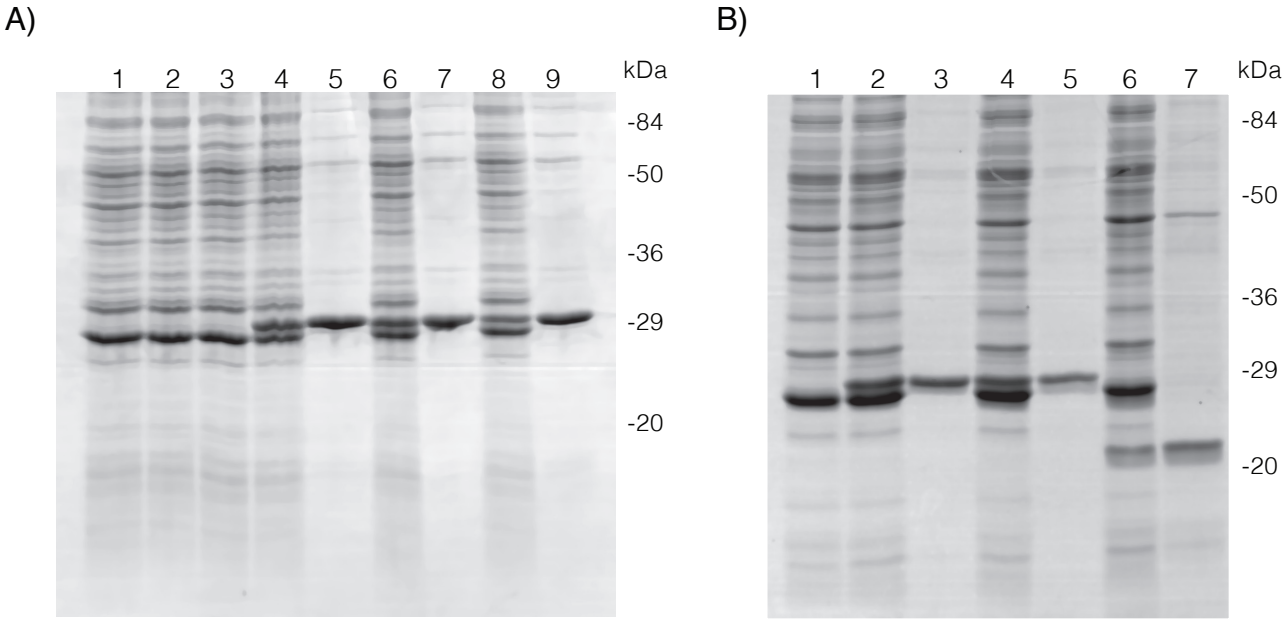

Figure S5. Expression of wild-type and SAMC variants in *E. coli* and their purification. (A) Protein extracts from *E. coli* expresssing control (BL-21 CodonPlus(DE3)-RIL expression vector) (lanes 1,3), wild-type (lanes 2, 4-5), p.Ala102Val (lanes 6-7) and p.Val148Gly (lanes 8-9) SAMC were separated by SDS PAGE and stained with Coomassie Blue. Samples were taken before (lanes 1 and 2) or 5h after (lanes 3, 4, 6 and 8) induction. Lanes 5, 7 and 9 represent purified SAMC (6.2 µg), p.Ala102Val SAMC (4.3 µg) and p.Val148Gly SAMC (4.7 µg) derived from bacteria shown in lanes 4, 6 and 8, respectively. (B) Protein extracts from *E. coli* expresssing control (BL-21 CodonPlus(DE3)-RIL expression vector) (lane 1), wild-type (lanes 2-3), p.Pro199Leu (lanes 4-5) and SAMCΔ1-88 (lanes 6-7) were analyzed as above. Samples were collected 5h after (lanes 1, 2, 4 and 6) induction. Purified samples for SAMC (3.6 µg), p.Pro199Leu SAMC (2.5µg) and SAMCΔ1-88 (3 µg) derived from bacteria shown in lanes 2, 4 and 6 are shown in lanes 3, 5 and 7, respectively.

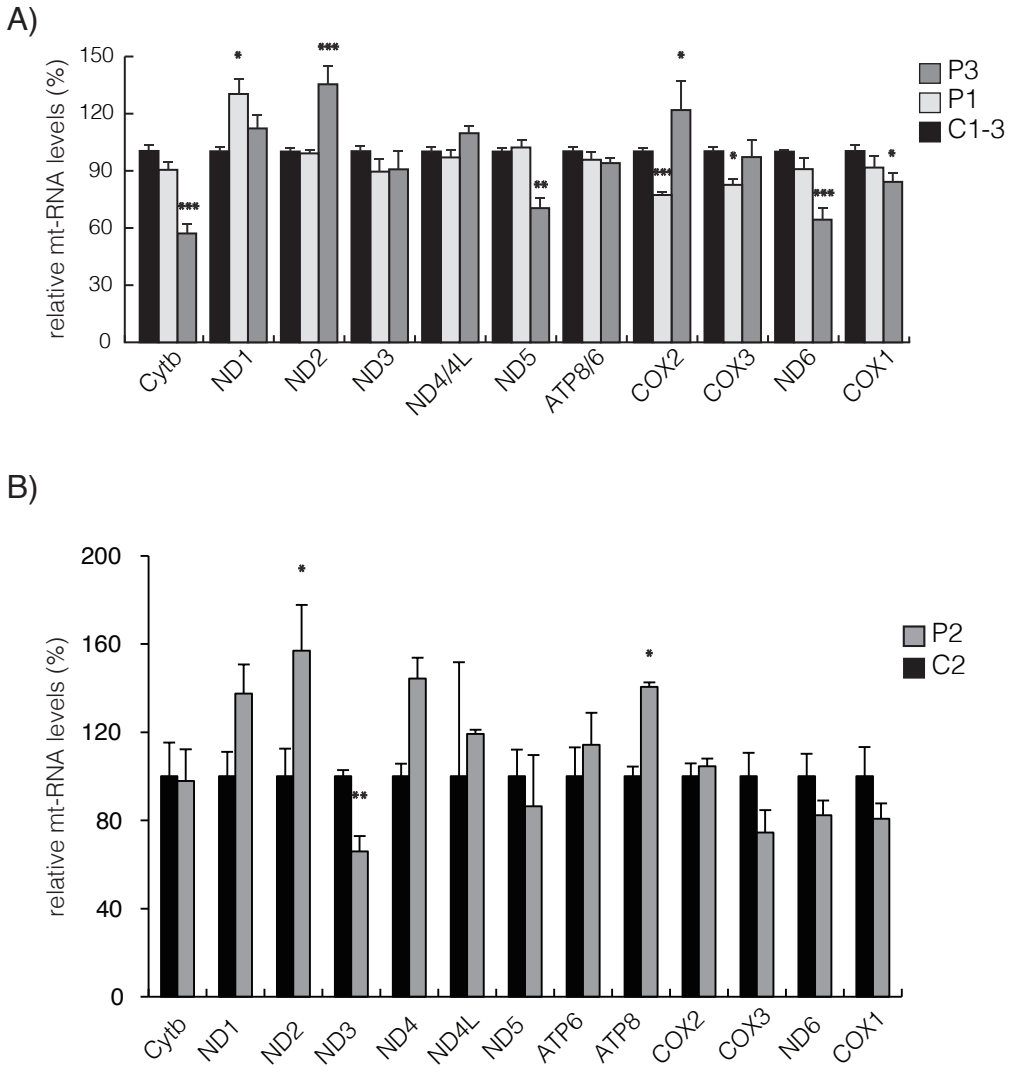

Figure S6: Steady-state levels of the indicated mitochondrial transcripts. Fibroblasts from (**A**) P1 and P3 or (**B**) P2 determined by qRT-PCR. All data are represented as mean ± SEM. (* $p<0.05$, ** $p<0.01$, ***$p<0.001$).